Electronic Supplementary Material (ESI) for Physical Chemistry Chemical Physics.

Supporting information for

Solvent Dependence of Excited-State Proton Transfer from Pyranine-derived Photoacids

Christian Spies[†], Shay Shomer[‡], Björn Finkler[†], Dina Pines[α], Ehud Pines[α*], Gregor Jung[†*] and Dan Huppert[‡*]

[‡]Raymond and Beverly Sackler Faculty of Exact Sciences, School of Chemistry,

Tel Aviv University, Tel Aviv 69978, Israel

[α]Department of Chemistry, Ben-Gurion University of the Negev, P.O.B. 653, Beer-Sheva 84105, Israel

[†]Biophysical Chemistry, Saarland University, Campus, Building B2 2, D-66123 Saarbruecken, Germany

Table S1. Reconvolution fitting of TCSPC data of **1a** in methanol using exponential functions.

λ [nm]	τ_1 [ns]	A_1	τ_2 [ns]	A_2	τ_3 [ns]	A_3	χ^2
460	0.14	0.88	0.48	0.10	3.21	0.02	1.66
470	0.10	0.78	0.32	0.20	2.58	0.02	1.17
480	0.13	0.88	0.45	0.10	2.70	0.02	1.61
490	0.13	0.89	0.45	0.10	2.55	0.01	1.27
500	0.12	0.85	0.39	0.14	2.41	0.01	1.36
510	0.13	0.85	0.40	0.14	3.25	0.01	1.23
520	0.13	0.86	0.47	0.12	4.76	0.02	1.15
530	0.09	0.62	0.29	0.31	5.85	0.07	1.20
540	0.14	0.50	0.31	0.14	6.12	0.36	1.12
550	0.72	0.45	0.92	-0.39	6.02	0.94	1.65
560	0.15	-0.34	6.12	0.95			1.34
570	0.13	-0.36	6.11	0.54			1.31
580	0.12	-0.47	6.09	0.73			1.35
590	0.13	-0.36	6.12	0.63			1.19
600	0.12	-0.40	6.11	0.75			1.38

Table S2. Reconvolution fitting of TCSPC date of **1b** in methanol using exponential functions.

λ [nm]	τ_1 [ns]	A_1	τ_2 [ns]	A_2	τ_3 [ns]	A_3	χ^2
440	0.14	0.42	1.54	0.36	4.51	0.22	1.05
450	0.17	0.31	1.59	0.43	4.55	0.26	1.06
460	0.18	0.26	1.62	0.46	4.59	0.28	1.23
470	0.14	0.23	1.60	0.49	4.59	0.28	1.50
480	0.11	0.21	1.64	0.51	4.72	0.28	1.43
490	0.14	0.13	1.53	0.52	4.44	0.35	1.26
500	0.09	0.16	1.52	0.50	4.48	0.34	1.92
510	0.18	0.16	1.66	0.49	4.65	0.35	1.05
520	0.19	0.14	1.58	0.32	4.57	0.54	1.19
530	0.31	0.13	0.82	-0.06	4.73	0.93	1.34

540	0.32	0.13	0.83	-0.07	4.73	0.94	1.34
550	1.62	-0.60	4.72	0.91			1.11
560	1.59	-0.53	4.75	0.73			1.12
570	1.57	-0.53	4.77	0.73			1.09

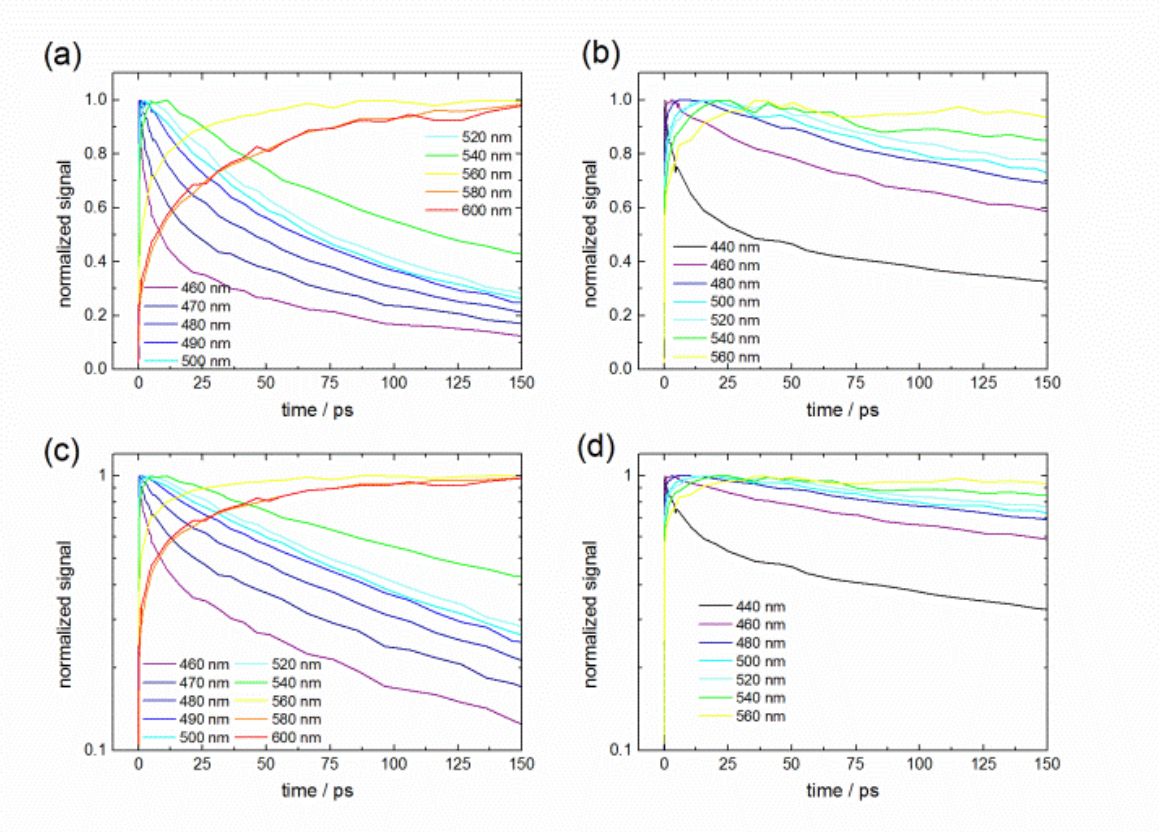

Figure S1. Up-conversion curves of **1a** (a) and **1b** (b) in methanol between 440 nm and 600 nm, on a linear and semi-logarithmic scale (c), (d).

Table S3. Reconvolution fitting of upconversion data of **1b** in methanol using exponential functions.

λ [nm]	τ_1 [ps]	A_1	τ_2 [ps]	A_2	τ_3 [ps]	A_3	χ^2
440	0.22	0.23	8.99	0.30	279	0.47	1.48
460	2.01	-0.03	31.9	0.19	440	0.84	4.69
480	2.79	-0.18	140	0.55	1500[a]	0.75	2.57
500	4.00	-0.25	150	0.37	1500[a]	0.58	2.84
520	4.21	-0.18	367	0.42	1500[a]	0.16	2.17
540	4.71	-0.19	183	0.09	1500[a]	0.46	1.62
560	1.00	-0.27	12.7	-0.64	1500[a]	1.98	1.38

[a] Variable fixed at this value.

Table S4. Reconvolution fitting of upconversion data of **1a** in methanol using exponential functions.

λ [nm]	τ_1 [ps]	A_1	τ_2 [ps]	A_2	τ_3 [ps]	A_3	χ^2
460	0.17	0.35	5.36	0.34	125	0.31	3.93
470	0.04	0.46	6.71	0.22	123	0.32	3.27
480	0.003	0.40	12.2	0.17	126	0.43	2.48
490	0.001	0.32	35.5	0.23	155	0.45	4.68
500	1.72	-0.07	62.2	0.72	319	0.35	3.48
520	2.17	-0.23	49.0	0.50	174	0.73	3.34
540	2.26	-0.20	101	0.54	6100[a]	0.17	2.59
560	2.28	-0.12	23.6	-0.15	6100[a]	0.44	2.23
580	3.32	-0.06	42.4	-0.16	6100[a]	0.27	3.99
600	0.99	-0.14	31.5	-0.33	6100[a]	0.57	3.15

[a] Variable fixed at this value.

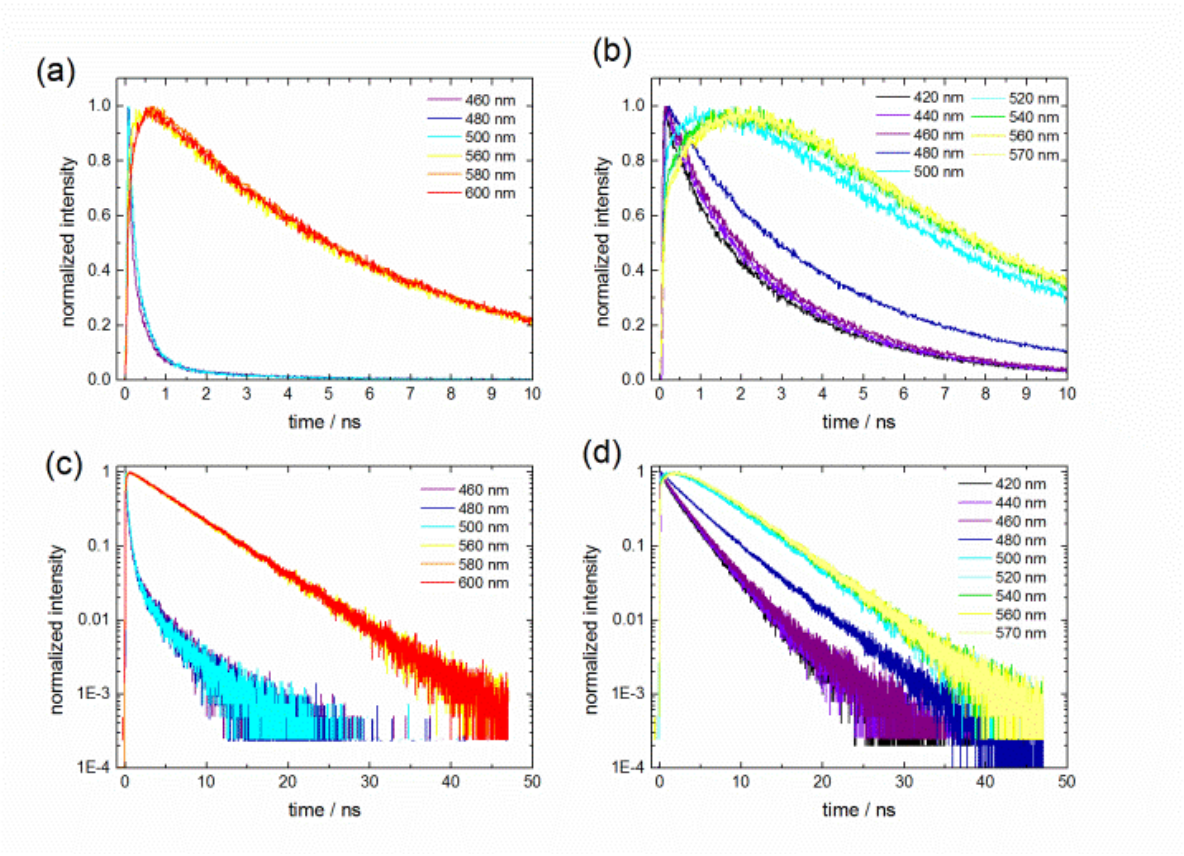

Figure S2. TCSPC curves of **1a** (a) and **1b** (b) in ethanol between 420 nm and 600 nm, on a linear and semi-logarithmic scale (c), (d).

Table S5. Reconvolution fitting of TCSPC data of **1b** in ethanol using exponential functions.

λ [nm]	**τ_1 [ns]**	**A_1**	**τ_2 [ns]**	**A_2**	**τ_3 [ns]**	**A_3**	**χ^2**
420	0.28	0.28	2.18	0.39	3.71	0.33	1.14
440	0.28	0.23	2.17	0.42	3.75	0.35	1.04
450	0.26	0.35	2.48	0.50	4.51	0.15	1.09
460	0.35	0.16	1.80	0.29	3.54	0.55	1.11
480	0.41	0.14	2.83	0.29	5.05	0.57	1.42
500	2.32	-0.31	5.24	0.55			1.32
520	2.28	-0.35	5.27	0.54			1.21
540	2.23	-0.36	5.28	0.54			1.16
560	2.16	-0.35	5.35	0.51			1.27
570	2.11	-0.35	5.37	0.50			1.26

Table S6. Reconvolution fitting of TCSPC date of **1a** in ethanol using exponential functions.

λ [nm]	τ_1 [ns]	A_1	τ_2 [ns]	A_2	τ_3 [ns]	A_3	χ^2
460	0.08	0.69	0.34	0.27	2.54	0.04	1.41
480	0.09	0.57	0.33	0.39	2.55	0.04	1.18
500	0.12	0.65	0.39	0.32	2.57	0.03	1.06
560	0.22	-0.19	5.98	1.01			1.10
580	0.20	-0.42	5.98	0.91			1.65
600	0.18	-0.27	6.01	0.62			1.14

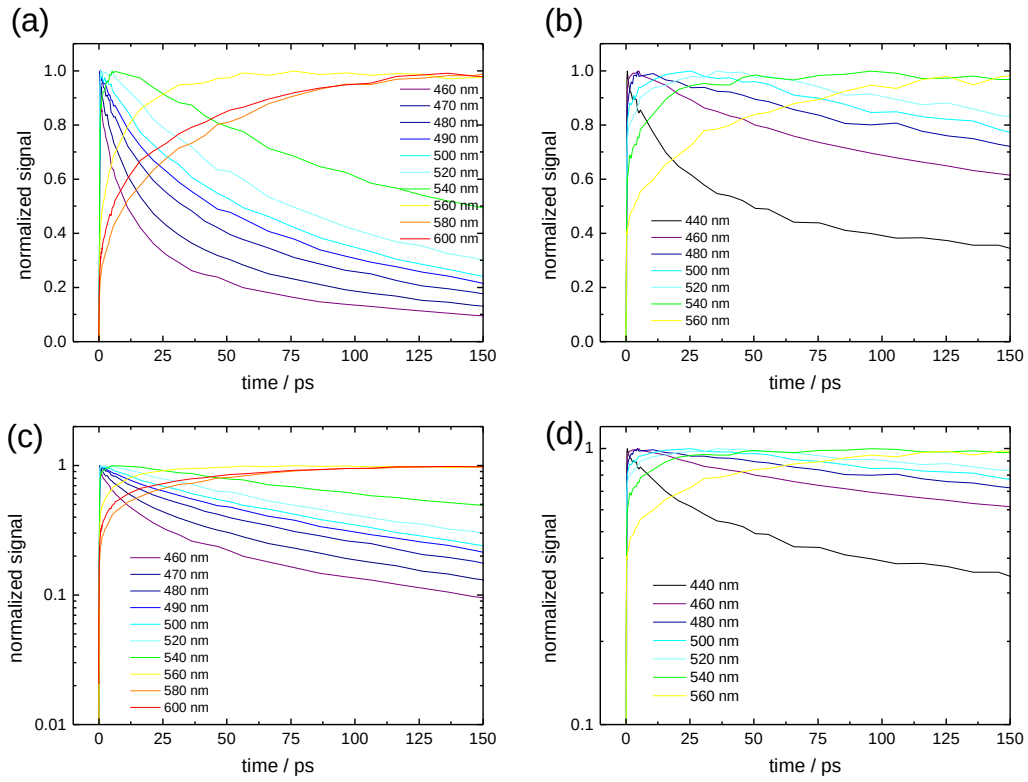

Figure S3. Up-conversion curves of **1a** (a) and **1b** (b) in ethanol between 440 nm and 600 nm, on a linear and semi logarithmic scale (c), (d).

Table S7. Reconvolution fitting of upconversion data of **1b** in ethanol using exponential functions.

λ [nm]	τ_1 [ps]	A_1	τ_2 [ps]	A_2	τ_3 [ps]	A_3	χ^{2_2}
440	0.05	0.40	20.6	0.27	369	0.33	1.25
460	2.35	-0.09	39	0.23	524	0.86	0.55
480	2.12	-0.12	175	0.42	5500[a]	0.49	2.93
500	7.63	-0.10	197	0.22	5500[a]	0.25	
520					5500[a]		
540	0.81	-0.02	13.4	-0.07	5500[a]	0.20	1.51
560	2.86	-0.12	44.5	-0.55	5500[a]	1.12	0.87

[a] Variable fixed at this value.

Table S8. Results of reconvolution fitting of upconversion data of **1a** in ethanol.

Wavelength	τ_1 [ps]	A_1	τ_2 [ps]	A_2	τ_3 [ps]	A_3	χ^2
460	0.06	0.52	9.3	0.29	114	0.19	4.65
470	0.07	0.38	12	0.32	121	0.3	2.87
480	0.003	0.5	16	0.21	131	0.29	3.08
490	0.003	0.46	20	0.19	143	0.35	1.65
500	0.003	0.4	29	0.21	158	0.39	2.98
520	3.4	-0.08	49	0.52	235	0.56	2.64
540	2.8	-0.02	1003		115	0.07	
560	1.1	-0.12	13	-0.38	6000[a]	0.78	2.86
580	2.5	-0.01	41	-0.04	6000[a]	0.07	4.11
600	0.18	-0.2434	5.46	-0.2653	6000[a]	0.07	2.28

[a] Variable fixed at this value.

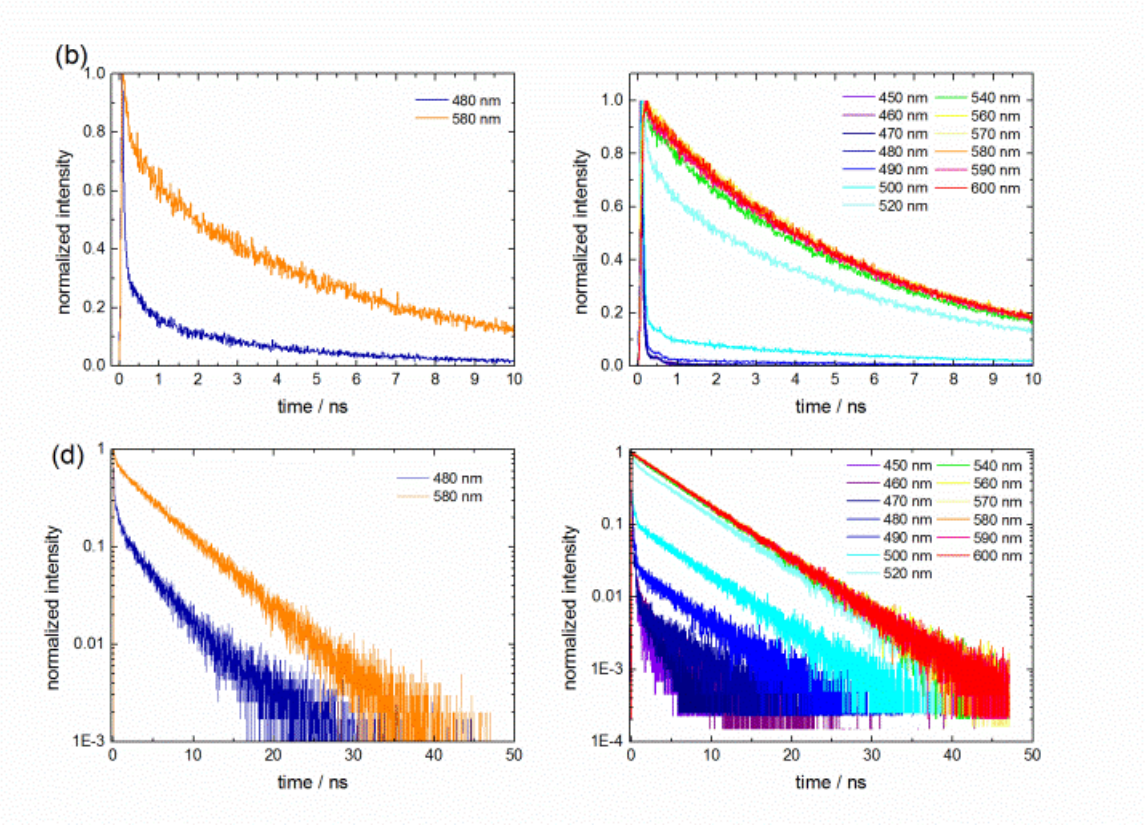

Figure S4. TCSPC curves of **1a** in 30 vol% water in methanol (a) and **1b** in water (b) between 450 nm and 600 nm, on a linear and semi-logarithmic scale (c), (d).

Table S9. Results of reconvolution fitting of upconversion data of **1b** in water.

Wavelength	**τ_1 [ps]**	**A_1**	**τ_2 [ps]**	**A_2**	**τ_3 [ps]**	**A_3**	**χ^2**
450	0.038	0.82	2.61	0.085	23.48	0.09	1.63
460	0.0032	0.79	4.46	0.143	34.09	0.06	5.17
470	0.349	0.37	12.68	0.54	70.3	0.09	1.53
480	0.274	0.267	13.11	0.623	71.28	0.11	1.4
490	0.43	0.162	15.4	0.743	100.76	0.095	1.56
550	4.15	-0.36	23.67	-0.31	594	1	1.18
560	0.982	-0.149	13.54	-0.627	616	1	1.18
570	4.37	-0.326	19.5	-0.411	673	1	0.83

Table S10. Results of reconvolution fitting of upconversion data of **1a** in water.

Wavelength	τ_1 [ps]	A_1	τ_2 [ps]	A_2	τ_3 [ps]	A_3	χ^2
460	0.30	0.54	3.58	0.40	152	0.06	2.52
470	0.49	0.47	4.90	0.47	113	0.07	5.29
480	0.73	0.43	6.78	0.52	105	0.05	7.37
490	1.30	0.40	9.09	0.52	143	0.08	4.42
520	0.77	0.15	9.06	0.68	142	0.17	2.11
540	1.10	-0.16	14.0	0.58	398	0.58	0.96
560	0.39	-0.41	4.67	-1.69	842		1.34
580	0.49	-0.58	5.70	-2.83	1005		1.23

Correction of pK_a values by electrostatic work term

The two new strong pyranine-derived photoacids shown in scheme 1 were found to have pK_a^* of ~ -4 (**1a**) and ~ -1 (**1b**) determined by the Förster cycle.[1] The ESPT rate of **1a** in water was measured to be 3×10^{11} s^{-1} (Table 2). The weaker photoacid, **1b,** exhibits a smaller ESPT rate as expected from the higher pK_a^* value. The ESPT rate constant of **1b** in water was found to be ~8×10^{10} s^{-1}. In comparison, the much studied parent (and also weaker) photoacid, the triply negatively charged HPTS molecule transfers a proton only in water with $k_{PT} \approx 10^{10}$ s^{-1}. We have correlated the HPTS photoacid together with the neutral photoacids after adjusting its pK_a^* value (1.4) to contact ion-pair formation rather than using the conventional value which include the electrostatic work needed to separate the ion pair to infinite separation distance, using eq. 7:

$$pK_a^* = pK^*(contact) + \frac{R_D}{2.3a} \quad (1)$$

where the Debye Radius R_D is given by eq. 8:

$$R_D = \frac{|z_1 z_2| e^2}{\varepsilon k_B T} \quad (8)$$

k_B is the Boltzmann constant, a = 6.5 Å is the reaction contact radius, ε is the permittivity of the solution, e is the elementary charge, and z_1 = 1, z_2 = -3 are the charge numbers of the proton and HPTS respectively. We find pK^*(contact) = 0 for HPTS and use this value for the free-energy correlation.

Sensitivity of change in proton transfer rate with pK_a^*

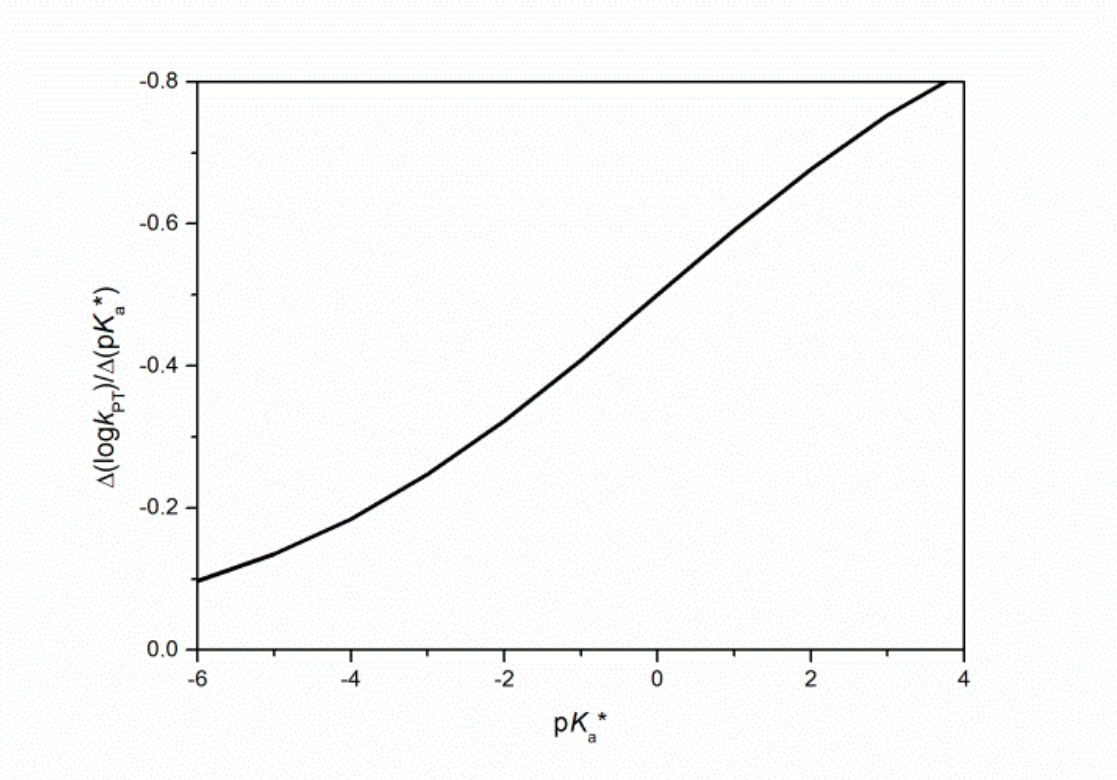

Figure S4. $\Delta(\log k_{PT})/\Delta(pK_a^*)$ of free-energy correlation found in the proton dissociation reaction (solid line in Fig. 11) vs pK_a^*.

In Fig. S4 we have plotted the derivative of the logarithm of the proton transfer rate k_{PT}, given by eqs. 2-5, as a function of the pK_a^*. This derivative of the Marcus free-energy function scales the sensitivity of the proton transfer rate to a pK^*_a change as a function of the absolute pK_a^* of the photoacid. The stronger the photoacid the less sensitive is the proton transfer rate to a pK^*_a change due to a solvent or a substituent change which do not alter the general mechanism of the proton transfer reaction in water. The derivative distinctly increases in the range of the acidities that were considered in this study (pK_a^* from -6 to 4) when moving from the stronger photoacids to the weaker ones and unambiguously reproduces the observed trend in the solvent effect on the dissociation rate of the photoacids.

Discussion of the wavelength dependence

As indicated in the manuscript, the strong wavelength dependence observed especially for compound **1b**, can have several reasons. In the manuscript we mention a quenching reaction competing with the ESPT reaction as a possible explanation for this finding. However, this may not be the solely answer to it. In fact, the values for the time constants in tables S9 and S10 are also varying with the wavelength. This could be due to the reconvolution fitting procedure and the non-exponential nature of solvation dynamics. In this case, the numbers in these tables may not be strictly correct, although the extraction of the ESPT rate should not be affected. Another possible explanation may be the vibrational structure of the bands. Due to the excitation at about 400 nm, higher vibrational levels are populated by the laser puls. Vibrational cooling may occur, although it usually should be completed within 10 ps, and hence have an impact in wavelength-resolved emission decays.